

New synthesis of quantum dots copper sulfide using the UV-irradiation technique

S. K. A. Hussein ^a, A. M. Rheima ^{*a}, F. F. AlKazaz ^a, S. H. Mohammed ^b,
I. K. I. Al-Khateeb ^c

^a Chemistry Department, College of Science, Mustansiriyah University, Baghdad, Iraq

^b Department of Chemistry, College of education, University of garmian, kalar, Iraq

^c Dijlah University College, Al-Masafi Street, Al-Dora, Baghdad 00964, Iraq

The article describes a new method for synthesizing quantum dots copper sulfide (CuS QDs) based on the UV-irradiation technique (photolysis method). Our process allows producing high-quality, small-size, very low cost and short time. The crystal structure of CuS QDs was characterized using X-ray diffraction (XRD) ,which confirmed the synthesized sample's hexagonal shape. The structure of the manufactured product was examined using energy-dispersive X-ray spectroscopy (EDX), and the result revealed just copper (Cu) and sulfide (S) elements, indicating that the synthetic material was pure. The morphology, optical properties, and particle size were investigated by photoluminescence spectroscopy (PL), scanning electron microscope (SEM), and transmission electron spectroscopy (TEM). The particles sizes of the CuS QDs were found to be range between 5.4 to 9.1 nm. Finally, this method successfully synthesized CuS QDs through the results.

(Received February 25, 2022; Accepted May 18, 2022)

Keywords: UV-Irradiation, Photolysis, QDs CuS, Photoluminescence

1. Introduction

Copper sulfide, whose chemical symbol is CuS, is a semiconductor with a high optical coefficient [1]. CuS is frequently employed in photothermal conversion [2-4], photocatalysis [5,6], and medicinal fields [7-9] due to its good physical and chemical properties. In addition, CuS nanomaterial offers many antimicrobial applications. CuS nanomaterial has antibacterial properties due to the following factors: (a) nano CuS can release Cu²⁺ in bacterial fluid with antibiotic properties [10], (b) CuS can convert near-infrared (N-IR) light into thermal energy due to the transition d-d band of Cu²⁺ [11], and (c) CuS nano - materials emit reactive oxygen species (ROS) when illuminated. As a result, our research focus has shifted to improving the three capacities while also improving the antibacterial properties of materials. The absorption limit of a single semiconductor material is frequently narrow [12], restricting its use in antimicrobial, hydrogen evolution, and degradation. As a result, various materials have been employed to construct nanomaterials to improve semiconductor materials' photocatalytic activity. Two-dimensional graphene [13,14] and MXenes materials [15-17] with "thin, wide, light, and strong" features are recommended for nanomaterials construction because they have a large aspect ratio, adjustable electrical characteristics, and necessary functional groups [18]. MXenes have a high conductivity as well [19]. MXenes can thus be used as carrier materials in the self-assembly of nanostructures [20,21] and can enhance semiconductor photocatalytic performance. Due to its superior performance has been used in various fields, including energy storage materials [22,23] and photoelectric fields [24,25]. Furthermore, MXenes are an effective photocatalytic material [26,27]. CuS is available in a variety of crystalline phases, including CuS (covellite), Cu₂S (chalcocite), Cu₇S₄-CuS (hexagonal plates), Cu₉S₅ (digenite octahedron), and Cu_{1.75}S (anilite) [28], making it a suitable semiconductor for biosensors [29] and gas sensors [30]. Copper sulfide is environmentally acceptable, inexpensive, non-toxic, easy to regenerate, biocompatible, and chemically stable, all of which contribute to its efficacy in eliminating dyes from wastewater

* Corresponding author: ahmed.rheima@gmail.com
<https://doi.org/10.15251/CL.2022.195.363>

[28,31,32]. The synthetic processes utilized to make CuS nanoparticles, such as hydrothermal, sol-gel, microemulsion, microwave, sonochemical, electrospinning, and single-source precursors, impact these properties [33-40]. It has been observed that employing a single-source precursor to make CuS nanoparticles produces high-quality nanoparticles due to the metal-sulfur relationship in the precursors [41,42]. This study produced the CuS QDs by a simple, low-cost, and convenient photocell-irradiated method, a straightforward and promising approach for our future.

2. Materials and methods

Copper acetate a $[\text{Cu}(\text{CH}_3\text{COO})_2 \cdot \text{H}_2\text{O}]$, sodium sulfate (Na_2S), urea (NH_2CONH_2) were obtained from Sigma-Aldrich. All the solutions were prepared in deionized water.

2.1. New Synthesis of Quantum dots Copper sulfide (QDs CuS)

QDs CuS was synthesized by a photolysis method [43,44]. The photo-cell comprises a 125 Watt of UV source (λ max of 365 nm) and an ice bath-cooled pyrex tube that prevents temperature rise caused by UV radiation (Figure 1). In a typical experimental procedure, copper acetate (0.01 mole, 1.95 gm) was dissolved in 100 ml of de-ionized water with a magnetically stirred. Then, 50 ml, 0.02 mole of urea was slowly added (drop by drop) to the copper solution and stirred for $\frac{1}{2}$ h. the mixture solution was irradiated in a photocell for 30 minutes. Then, 50ml of 0.01 mole sodium sulfate was added slowly to the solution. A black powder was precipitated and washed several times using de-ionized water. The final material dried at room temperature to obtain a black powder CuS sample.



Fig. 1. photo-cell of Synthesis QDs CuS.

2.2. Characterization of QDs CuS

Several devices determined QDs CuS powder, X-ray diffraction powder (XRD) was achieved using (Model D-5000) with a λ of 0.154 nm. Field emission scanning electron microscope (FE-SEM) model Jeol JSM-6010LV was used to determine the morphology and topography of the prepared sample. Transmission electron microscopy (TEM) type JEOL JEM-2100 was used to investigate the shape and size of QDs CuS powder. Photoluminescence measurements (PL) emission measured was used to determine the optical properties of QDs CuS.

3. Results and Discussion

XRD analysis was used to determine the crystal structure of the produced sample. Figure 2 shows the XRD pattern of the Copper sulfide powder, with peaks at $2\theta = 29.2, 31.8, 32.7, 48.0, 52.7,$ and 59.2 attributed to hexagonal CuS crystal facets (102), (103), (006), (110), (108), and (116) [45]. The measured peaks, which lacked any confusing peaks, were closely matched with the Copper sulfide in phase CuS according to the standard JCPDS card (No. 06-0464), indicating that the CuS product has only one phase. The Debye-Scherrer formula was used to estimate the crystal structure of QDs CuS [43,44]:

$$D = k\lambda / \beta \cos \theta$$

where D = crystal size, $K = 0.9$ (Scherrer constant), $\lambda = 0.154$ nm (wavelength of Cu-K radiations), β is the complete width at half maximum, and theta (θ) is the angle calculated from two values matching to the XRD pattern. The crystallite size was 9.14 nm.

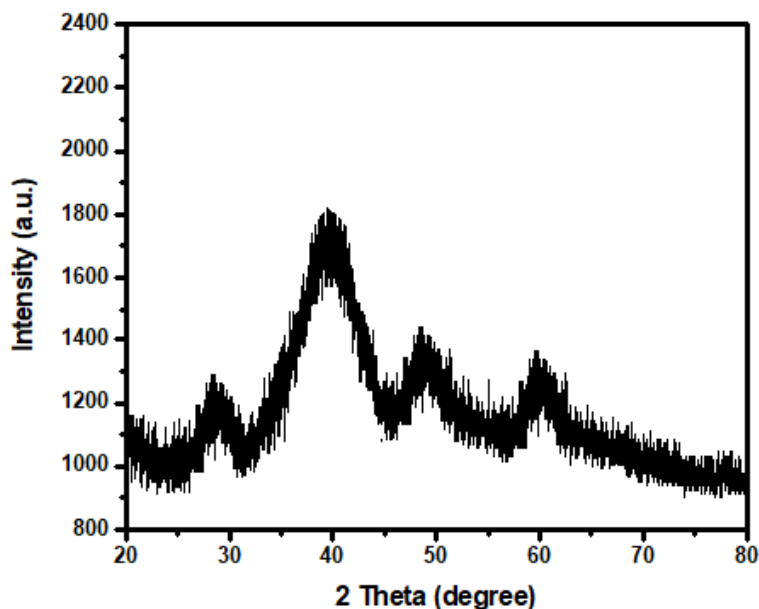


Fig. 2. XRD pattern of QDs CuS.

The EDX technique was used to determine the chemical composition of CuS. Figure 3 shows the resulting spectrum, demonstrating that only Cu and S were present. The percentage amount of Cu and S was shown in the inner table. The two elements' molar ratio was determined to be 1:1, consistent with the theoretical CuS ratio. The discovery confirmed that the CuS crystal phase was present in the sample produced.

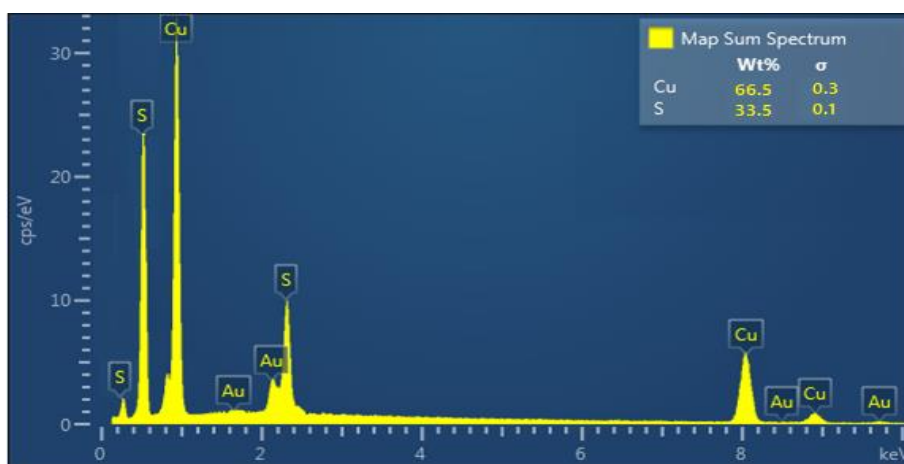


Fig. 3. EDX spectrum of QDs CuS.

The corresponding EDS elemental mapping pictures of Cu and S with a 1:1 ratio are shown in Figure 4. The Cu and S components can be seen uniformly scattered on the sample's surface, supporting the catalyst elements' dispersion.

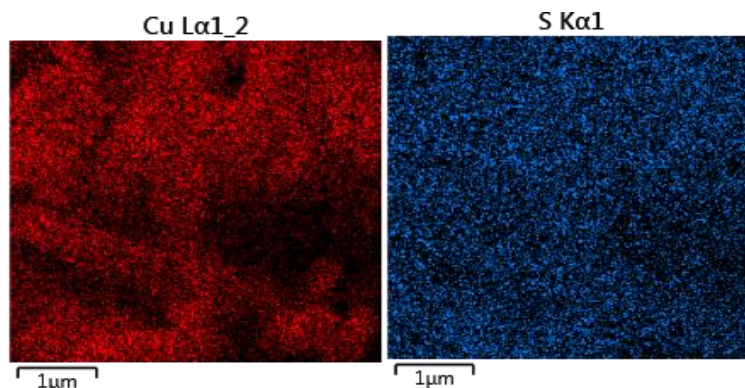


Fig. 4. EDX elemental mapping images of Cu and S elements.

TEM images studied the shape and size of the CuS sample (Figure 5). This TEM image absence of aggregates due to the presence of urea as a surfactant and the efficiency of the photolysis method. Interestingly, the CuS sample contains uniform quantum dots (QDs) with narrow particle size ranges that are well-dispersed (5.4 to 9.1 nm). The hexagonal shape is apparent in the images. This was very similar to the XRD result.

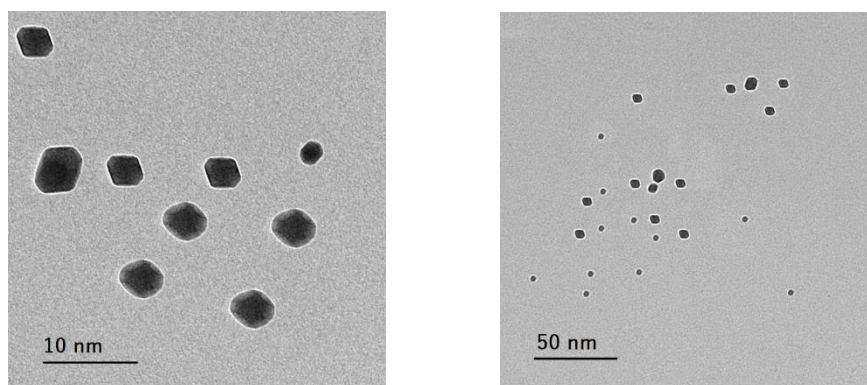


Fig. 5. TEM image of QDs CuS.

The surface shape and particle size of the CuS QDs produced were examined using FESEM experiments. Figure 6 shows the typical FESEM for this sample. The micrographs show that the samples have a good crystalline structure, as evidenced by the prominent display of lattice fringes. The QDs were well dispersed, spherical, and monodisperse (zero-dimensional) without aggregation (all dimensions are less than 100 nm). The FESEM test demonstrates that the QDs have a spherical morphology. A TEM examination was conducted to record TEM images of samples to understand the particle size of QDs better.

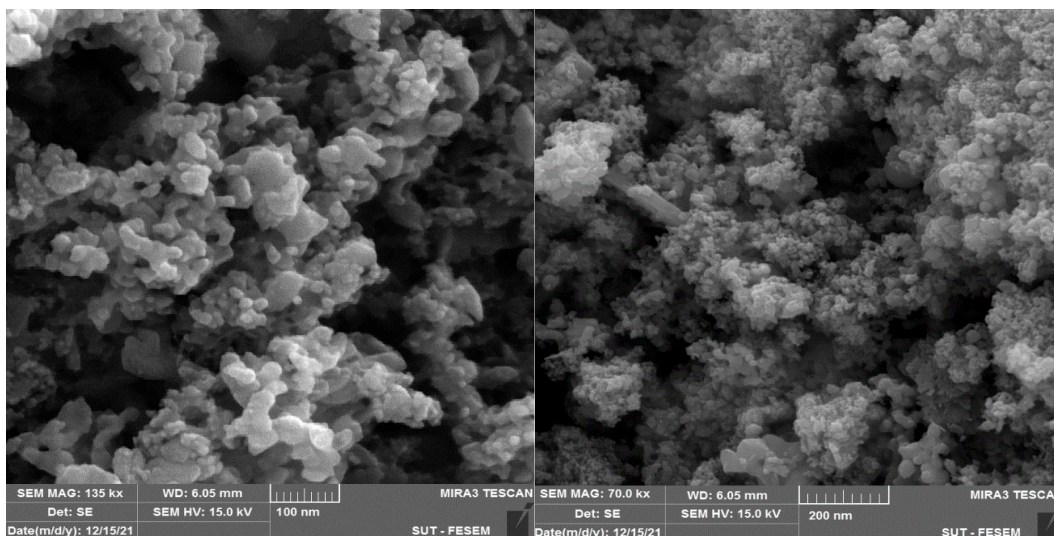


Fig. 6. SEM images of QDs CuS.

The charge carrier dynamics of QDs CuS were investigated using the photoluminescence (PL) quenching spectra. CuS QDs contain two peaks in their PL spectra, at 353 and 728 nm (Figure 7). They recombine the sulfur-vacancy-related donor and the valence band peaks at 353 nm. The CuS trap state emission, related to copper's origin vacancy, is responsible for the emission peak of 728 nm. Meanwhile, CuS has a lower PL intensity than other samples in the literature [46], preventing light-excited charges from recombining and speeding up transport. The spectra show blue peaks that are notably different from those found in bulk samples, indicating a quantum size effect. The quantum dots exhibit quantum-confined effects and size-tuned optical properties due to this property. The lifetime of photo-generated electrons is increased. CuS can efficiently minimize photo-excited charge carrier recombination, according to PL experiments [47].

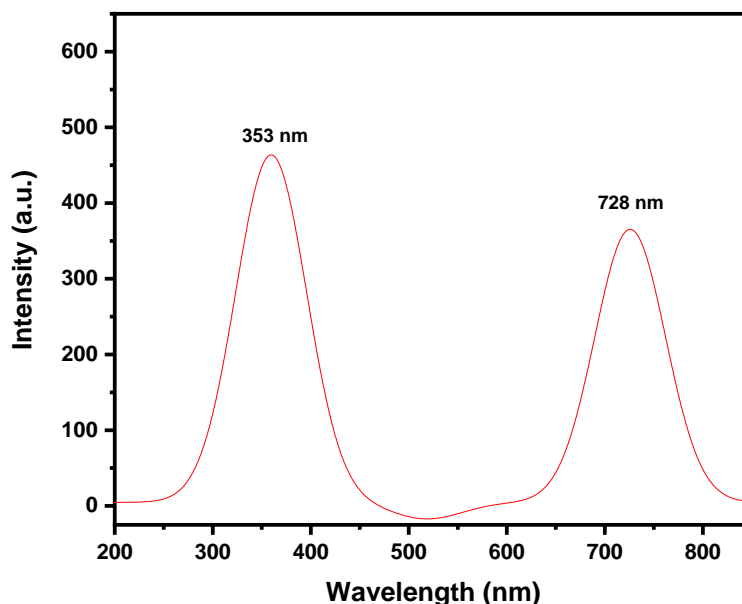


Fig. 7. PL spectrum of QDs CuS.

4. Conclusion

In conclusion, quantum dots CuS has been successfully synthesized by photolysis method (UV-Irradiation method), which is considered a novelty. XRD patterns confirmed the production of covellite with hexagonal phases in structures. SEM and TEM studies demonstrated less polydispersity for particles with a diameter of 5.4 to 9.1 nm. CuS QDs PL curves show a large absorption band on the visible region between 353 and 728 nm, which has a higher intensity in the sample. These findings indicate that the quantum dots created could be helpful in various applications, including buffer layers for solar cells, catalysts, sensors, biological labeling, and optical materials.

References

- [1] Bhatt, Vishwa; Kumar, Manjeet; Yun, Ju-Hyung, *Journal of Alloys and Compounds*, 2022, 891: 161940; <https://doi.org/10.1016/j.jallcom.2021.161940>
- [2] Tian, J., Zhang, W., Gu, J., Deng, T., & Zhang, D. (2015), *Nano Energy*, 17, 52-62; <https://doi.org/10.1016/j.nanoen.2015.07.027>
- [3] Zhang, Xiaohui, et al., *Chemical Engineering Journal*, 2020, 388: 124304; <https://doi.org/10.1016/j.cej.2020.124304>
- [4] Mathew, Sheril Ann, et al., *Journal of Drug Delivery Science and Technology*, 2021, 61: 102193; <https://doi.org/10.1016/j.jddst.2020.102193>
- [5] Varghese, Jini, *Journal of Physics and Chemistry of Solids*, 2021, 156: 109911; <https://doi.org/10.1016/j.jpcs.2020.109911>
- [6] Zhang, Fan, et al., *Catalysis Today*, 2019, 330: 203-208; <https://doi.org/10.1016/j.cattod.2018.03.060>
- [7] Poudel, Kishwor, et al., *International journal of pharmaceutics*, 2019, 562: 135-150; <https://doi.org/10.1016/j.ijpharm.2019.03.043>
- [8] Xu, Mengshu, et al., *Chemical Engineering Journal*, 2019, 360: 866-878; <https://doi.org/10.1016/j.cej.2018.12.052>
- [9] Costa, Elizangela P., et al., *Chemical Engineering Journal*, 2020, 385: 123982; <https://doi.org/10.1016/j.cej.2019.123982>
- [10] Liu, Xiao-Fei, et al., *Chemical Engineering Journal*, 2020, 401: 126096; <https://doi.org/10.1016/j.cej.2020.126096>
- [11] Ding, Hongyan, et al., *Journal of hazardous materials*, 2020, 393: 122423; <https://doi.org/10.1016/j.jhazmat.2020.122423>
- [12] Zhao, Chen, et al., *Chemical Engineering Journal*, 2021, 417: 128022; <https://doi.org/10.1016/j.cej.2020.128022>
- [13] Hu, Yumeng, et al., *Chemical Engineering Journal*, 2021, 414: 128795; <https://doi.org/10.1016/j.cej.2021.128795>
- [14] Ozer, Lütfiye Yıldız, et al., *Journal of Photochemistry and Photobiology C: Photochemistry Reviews*, 2017, 33: 132-164; <https://doi.org/10.1016/j.jphotochemrev.2017.06.003>
- [15] Naji, Amel, et al., *Materials Letters*, 2022, 322: 132473; <https://doi.org/10.1016/j.matlet.2022.132473>
- [16] Rheima, Ahmed Mahdi, et al., *Digest Journal of Nanomaterials and Biostructures*, 2021, 16: 11-18; https://chalcogen.ro/11_RheimaAM.pdf
- [17] Kadhum, Haider A , et al., *Applied Physics A*, 2020, 126: 802; <https://doi.org/10.1007/s00339-020-03985-6>
- [18] Rheima, Ahmed Mahdi, et al., *IOP Conference Series: Materials Science and Engineering*, 2020, 928: 052036; <https://doi.org/10.1088/1757-899X/928/5/052036>

- [19] Kamil, Amal Fadhil, et al., Journal of Ovonic Research, 2021, 815: 299-305;
https://chalcogen.ro/299_KamilAF.pdf
- [20] Rheima, Ahmed Mahdi, et al., Nano Biomed. Eng, 2021, 13: 1-5;
<https://doi.org/10.5101/nbe.v13i1.p1-5>
- [21] Rasheed, Tabinda, et al., Advanced Powder Technology, 2021;
<https://doi.org/10.1016/j.appt.2021.05.006>
- [22] WU, Yuanji, et al., Chemical Engineering Journal, 2021, 404: 126565;
<https://doi.org/10.1016/j.cej.2020.126565>
- [23] Zhu, Qizhen, et al., Energy Storage Materials, 2021, 35: 630-660;
<https://doi.org/10.1016/j.ensm.2020.11.035>
- [24] Deshmukh, Kalim; Kovářik, Tomáš; Pasha, SK Khadheer, Coordination Chemistry Reviews, 2020, 424: 213514; <https://doi.org/10.1016/j.ccr.2020.213514>
- [25] Zhu, Xiaohua, et al., Biosensors and Bioelectronics, 2021, 171: 112730;
<https://doi.org/10.1016/j.bios.2020.112730>
- [26] Hong, Long-fei, et al., Materials Today Energy, 2020, 100521;
<https://doi.org/10.1016/j.mtener.2020.100521>
- [27] Feng, Xiaofang, et al., Ceramics International, 2021, 47.6: 7321-7343;
<https://doi.org/10.1016/j.ceramint.2020.11.151>
- [28] Shamraiz, Umair, et al., Journal of Saudi Chemical Society, 2017, 21.4: 390-398;
<https://doi.org/10.1016/j.jscs.2015.07.005>
- [29] Rubilar, Olga, et al., Biotechnology Letters, 2013, 35.9: 1365-1375;
<https://doi.org/10.1007/s10529-013-1239-x>
- [30] Aboud, Nibras Abdul Ameer, et al., Chalcogenide Letters, 2021, 18: p. 237 - 243;
- [31] Srinivas, Billakanti; Kumar, Baskaran Ganesh; Muralidharan, Krishnamurthi, Journal of Molecular Catalysis A: Chemical, 2015, 410: 8-18; <https://doi.org/10.1016/j.molcata.2015.08.028>
- [32] Kamil, Amal Fadhil, et al., Journal of Ovonic Research, 2021,17, p253-259;
https://chalcogen.ro/253_KamilAF.pdf
- [33] Rheima, Ahmed Mahdi, et al., Journal of Nanostructures, 2021, 11: p.609-617;
<https://doi.org/110.22052/JNS.2021.03.018>
- [34] Zhou, Xiuquan; Soldat, Anne Christine; Lind, Cora, RSC Advances, 2014, 4.2: 717-726;
<https://doi.org/10.1039/C3RA45053H>
- [35] Song, Xinyu, et al., Journal of colloid and interface science, 2004, 273.2: 463-469;
<https://doi.org/10.1016/j.jcis.2004.01.019>
- [36] Jeyabanu, K., et al., Physica B: Condensed Matter, 2019, 573: 92-101;
<https://doi.org/10.1016/j.physb.2019.08.028>
- [37] Singh, Alok; Manivannan, R.; Victoria, S. Noyel, Arabian Journal of Chemistry, 2019, 12.8: 2439-2447; <https://doi.org/10.1016/j.arabjc.2015.03.013>
- [38] Xu, Jia, et al., Bulletin of Materials Science, 2008, 31.2: 189-192;
<https://doi.org/10.1007/s12034-008-0033-1>
- [39] Ajibade, Peter A.; Botha, Nandipha L., Results in physics, 2016, 6: 581-589;
<https://doi.org/10.1016/j.rinp.2016.08.001>
- [40] Ajibade, Peter A., et al., Journal of Molecular Structure, 2020, 1221: 128791;
<https://doi.org/10.1016/j.molstruc.2020.128791>
- [41] Dojer, Brina, et al., Journal of Molecular Structure, 2019, 1194: 171-177;
<https://doi.org/10.1016/j.molstruc.2019.05.047>
- [42] Ajibade, Peter A., et al., Chemical Physics Letters, 2020, 755: 137813;
<https://doi.org/10.1016/j.cplett.2020.137813>
- [43] Kamil, Amal Fadhil, et al., Egyptian Journal of Chemistry, 2021, 64.11: 5-6;
<https://doi.org/10.21608/ejchem.2021.66737.3437>
- [44] Rheima, Ahmed, et al., Iranian Journal of Physics Research, 2020, 20.3: 51-55;
<https://doi.org/10.47176/ijpr.20.3.38771>

- [45] Zhong R, Peng C, Chen L, Yu N, Liu Z, Zhu M, He C, Chen Z., RSC advances. 2016;6(46):40480-8; <https://doi.org/10.1039/C5RA26801J>
- [46] Wang, Peipei, et al., ACS applied materials & interfaces, 2016, 8.24: 15820-15827; <https://doi.org/10.1021/acsami.6b04378>
- [47] Du W, Liao L, Yang L, Qin A, Liang A., Scientific reports. 2017 Sep 13;7(1):1-2; <https://doi.org/10.1038/s41598-017-10904-y>